

Mouse Endocrine Gland-Derived Vascular Endothelial Growth Factor: A Distinct Expression Pattern from Its Human Ortholog Suggests Different Roles as a Regulator of Organ-Specific Angiogenesis

JENNIFER LECOATER, RUI LIN, GRETCHEN FRANTZ, ZEMIN ZHANG, KENNETH HILLAN, AND NAPOLEONE FERRARA

Departments of Molecular Oncology (J.L., R.L., N.F.), Pathology (G.F., K.H.), and Bioinformatics (Z.Z.), Genentech Inc., South San Francisco, California 94080

We recently described human endocrine gland-derived vascular endothelial growth factor (EG-VEGF) as an endothelial cell mitogen with a novel selective activity and an expression pattern essentially limited to steroidogenic glands. Herein we present the identification and characterization of the mouse ortholog. The mouse cDNA and predicted amino acid sequences are, respectively, 86% and 88% identical with the human. Surprisingly, the mouse EG-VEGF transcript is predominantly expressed in liver and kidney. A comparison of human and mouse EG-VEGF promoter sequences revealed a potential binding site for NR5A1, which is known to be a pivotal element for steroidogenic-specific transcription, in the human but not

mouse promoter. *In situ* hybridization studies localized expression of mouse EG-VEGF mRNA to hepatocytes and renal tubule cells. Interestingly, capillary endothelial cells in these sites share several common structural features with those found in steroidogenic glands. Within liver and kidney, EG-VEGF receptor expression was largely restricted to endothelial cells. Mouse EG-VEGF promoted proliferation and survival of endothelial cells. We propose that mouse EG-VEGF, like human EG-VEGF, plays a role in regulating the phenotype and growth properties of endothelial cells within distinct capillary beds. (*Endocrinology* 144: 2606–2616, 2003)

ANGIOGENESIS IS A COMPLEX process, initially responsible for pruning and reorganizing the primitive capillary plexus of the developing embryo (1). In the adult, angiogenesis is restricted to and required for reproductive function and wound healing. Several angiogenic factors with otherwise pleiotropic activities have been reported including hepatocyte growth factor, the acidic and basic fibroblast growth factors, and IL-8 (2). The requirements for the endothelial cell-specific angiogenic factors vascular endothelial growth factor (VEGF; Refs. 3 and 4) and the angiopoietins (5, 6), and their cognate receptors (7–9), were demonstrated in a series of genetic studies in the mouse. Although VEGF and the angiopoietin molecules are essentially selective for endothelial cells, they are widely expressed. Therefore, it has been difficult to reconcile endothelial cell phenotypic diversity with the action of these ubiquitous factors. Although the molecular nature of tissue-specific factors shaping these characteristics has been undefined, presumably a complex network of secreted or cellular factors function as determinants. Moreover, that tissue capillaries are distinct and these cells express unique vascular addresses has given rise to new

approaches aimed at targeting tissues, via capillary-selective antigens (10, 11).

We reported previously the identification of a novel human endothelial cell mitogen, designated endocrine gland-derived VEGF (EG-VEGF; Ref. 12). Human EG-VEGF (hEG-VEGF) mRNA expression is restricted to steroidogenic cells, and EG-VEGF is an endothelial cell mitogen selective for endocrine gland endothelium (12).

EG-VEGF is a member of a structurally related class of peptides including the digestive enzyme colipase, the *Xenopus* head-organizer, dickkopf (13); venom protein A (VPRA; Ref. 14); or mamba intestinal toxin-1 (15), a nontoxic component of *Dendroaspis polylepis polylepis* venom; and the secreted protein from *Bombina variegata*, designated Bv8 (16). The distinguishing structural motif is a colipase-fold, 10-cysteine residues that form 5 disulfide bridges within a conserved span (17). EG-VEGF (80% homologous to VPRA) and VPRA are most closely related (83 and 79% homology) to the Bv8 peptide. Mammalian orthologs of Bv8 (Ref. 18; also known as prokineticin-2, Ref. 19) have been recently described and several activities for these proteins have been reported, including effects on neuronal survival (20), gastrointestinal smooth muscle contraction (19), and circadian locomotor rhythm (21). We recently demonstrated that delivery of Bv8 or EG-VEGF in the testis elicits an indistinguishable angiogenic response (22). Recently, two cognate G protein-coupled receptors for EG-VEGF and Bv8 have been identified (23, 24). These proteins are 80–90% identical and belong to the neuropeptide Y receptor family.

To further characterize the function and biology of EG-

Abbreviations: aa, Amino acids; ACE, adrenal cortex capillary endothelial; BAC, bacterial artificial chromosome; C/EBP, CCAAT enhancer binding protein; EG-VEGF, endocrine gland-derived vascular endothelial growth factor; EG-VEGFR-1, EG-VEGF receptor 1; EG-VEGFR-2, EG-VEGF receptor 2; FCS, fetal calf serum; HBSS, Hanks' balanced salt solution; hEG-VEGF, human EG-VEGF; LSEC, liver sinusoidal endothelial cells; mEG-VEGF, mouse EG-VEGF; SF, steroidogenic factor; VPRA, venom protein A.

VEGF, we cloned the mouse ortholog and examined its expression and activity. Although the predicted mature EG-VEGF peptide is 88% identical with the human sequence, a striking difference exists in this molecule's expression pattern, being predominantly expressed in the kidney and liver. These genes are syntenic and the gene organization is conserved, although the promoter sequences have diverged reflecting unique transcriptional regulation. Recombinant mouse EG-VEGF (mEG-VEGF) promoted the growth and survival of primary mouse liver sinusoidal endothelial cells (LSEC) as well as bovine adrenal cortex endothelial cells. Therefore, although mEG-VEGF is expressed at distinct tissue sites relative to the human ortholog, the biological activities appear to be analogous, due to the selective coexpression of an EG-VEGF receptor in the vascular endothelium.

Materials and Methods

Mouse EG-VEGF cDNA and gene cloning

An expressed sequence tag (GenBank accession no. BC9730410) derived from mouse kidney, highly related to human EG-VEGF, was identified in the public database. This fragment was amplified from a mouse kidney cDNA library and subsequently used as a probe for isolating the full-length cDNA. For colony hybridizations, 50 ng of the fragment corresponding to the expressed sequence tag served as the template for the random priming reaction, Rediprime II with 50 μ Ci of α -³²P-deoxy-CTP. The probe was hybridized to the library filters in hybridization solution (5 \times Denhardt's reagent, 50 mM sodium phosphate, 250 μ g/ml sheared herring sperm DNA, 6 \times saline sodium citrate, and 0.5% sodium dodecyl sulfate), washed at 68 C with 0.2 \times saline sodium citrate and 0.1% sodium dodecyl sulfate for 30 min and exposed to Kodak (Rochester, NY) XAR film for 1–16 h.

Primers to amplify the predicted exon 2 were used to identify bacterial artificial chromosome (BAC) clones from the Research Genetics, Inc. (Huntsville, AL) Sv129J library. All mouse cDNA and genomic clones were sequenced in their entirety. Mouse promoter sequence matches GenBank accession no. NW000200.1. hEG-VEGF gene sequence was obtained from GenBank (accession no. NT-019273) and compared with Celera data. Promoter analysis of the human and mouse sequences was performed using the alignment and search resources (Genentech, Inc.). For chromosomal assignments, the mouse gene was mapped to chromosome 3 using National Center for Biotechnology Information data, and EG-VEGF and known flanking genes on chromosome 1p13.1 (Locus Link) were compared with the mouse syntenic data.

Expression analyses

For Northern blot analysis, the probe (the full-length coding region) was hybridized to the mouse tissue blot (CLONTECH Laboratories, Inc., Palo Alto, CA) as described above. Total RNA was isolated from mouse liver, ovary, prostate, purified hepatocytes, liver, and kidney endothelial cells using the RNeasy kit according to the manufacturer's instructions. Taqman or real-time RT-PCR analysis was performed as previously described (12). Briefly, 50 ng of total RNA was used in each reaction. Mouse ovary or liver sample was used to generate standard curves, and all data were normalized to the mouse glyceraldehyde-3-phosphate dehydrogenase transcript level, therefore resulting in a relative transcript level. Primer and probe sequences used are as follows: mEG-VEGF: forward 5'-TGAGGAAACGCCAACACCAT, reverse 5'-CCGG-GAACCITGGAGCAC; probe FAM-CCTGTCCCTGCTCACCACAGC-CTG-TAMRA; mBv8: forward CCGAGGATGCACACACAC, reverse CCGGTTGAAAGAAGTCCTTAACA, probe FAM-CCCCTGCCTGCC-CAGGCTTGG-TAMRA; mVEGF: forward TTGACCTAGTCTCATGG-TAAAGC, reverse TCACTGAACCTGGGAATCAC, probe FAM-ACA-TTTCATGCAATGGCGGCT-TAMRA; mEG-VEGF/Bv8R-1: forward CAGCGCACATGAAGACTTG, reverse GTCATCTTCGGTTTCCT-CAGT, probe FAM-TCCAGGCAGCACCCCTGATG-TAMRA; mEG-VEGF/Bv8R-2: forward GAACTCCACCTGAGCGCA, reverse GGG-

TCCCATGTTGATGATGCT, probe FAM-CTCCCTGATACACACCA-GCCACCTG-TAMRA; mouse glyceraldehyde-3-phosphate dehydrogenase: forward ATGTTCCAGTATGACTCCACTCACC, reverse GAA-GACACCAGTAGACTCCACGACA, probe FAM-AAGCCCATCAC-CATCTTCCAGGAGCGACA-TAMRA. All analyses were replicated with at least two independent source materials.

Tissues were processed for *in situ* hybridization (25) and ³³P-uridine triphosphate-labeled RNA probes were generated by methods previously described (26). Sense and antisense probes were synthesized from a cDNA fragment corresponding to the first 509 nucleotides.

Recombinant protein production

The nucleotide sequence corresponding to the mature mEG-VEGF peptide was cloned into the pSecTag2/Hygro myc-epitope/his6 vector (Invitrogen, San Diego, CA). This construct was sequence verified and subsequently transfected using Effectene (QIAGEN, Valencia, CA) into 293T cells plated on poly D-lysine-coated plates. After an overnight incubation, growth media were replaced with DMEM supplemented with 0.2% BSA (Sigma, St. Louis, MO). Media were collected over the following 4 d, and recombinant protein was purified via its myc tag with antibody-coupled resin. Recombinant human EG-VEGF, a his-tagged baculovirus-produced protein previously described (12), and recombinant *Escherichia coli*-produced VEGF (Genentech, Inc.) were also used in cell assays.

Endothelial cell isolation

Livers were perfused in a retrograde fashion according to a previously described procedure (27) with Hanks' buffered saline [Hanks' balanced salt solution (HBSS) without calcium and magnesium] supplemented with 2 mM EDTA. After 5 min, livers were perfused with 0.5% collagenase type IV (Sigma) in complete HBSS for an additional 10–12 min. Tissues and cells were subsequently processed as previously described (28). Briefly, tissue was minced and passed through 40- μ m cell strainers, and hepatocytes were depleted with two low-speed centrifugations. The remaining nonparenchymal cells were washed and incubated on ice with 1 μ g of biotinylated antimouse CD31 (MEC 13.3) (PharMingen, San Diego, CA) for every 10⁶ cells. Subsequently, the cells were washed and incubated with streptavidin-coupled paramagnetic beads (Miltenyi Biotec, Auburn, CA) and applied to an LS+ column in the Vario magnetic-activated cell sorting magnet. The identity and purity (>98%) of endothelial cells was verified by fluorescence-activated cell sorting analysis for CD31, CD34 (PharMingen), and Flk-1 (Genentech, Inc.), and uptake of 1,1'-dioctadecyl-3,3',3'-tetramethylindocarbocyanine perchlorate-labeled acetylated low-density lipoprotein (Biomedical Technologies Inc., Stoughton, MA; Ref. 28). The purified endothelial cells were immediately processed for RNA isolation or plated in 6-well or 24-well dishes, previously coated with a 0.002% solution of fibronectin, in CSC medium with serum and growth factors (Cell Systems, Kirkland, CA) and supplemented with an additional 5 ng/ml recombinant VEGF. Cells were passaged, four donor samples were pooled, and 1–3 \times 10⁶ cells were plated in each well of a duplicate 6-well dish for assays. Kidney endothelial cell preparations were obtained using the same reagents as described above. Briefly, the mouse was perfused through the left ventricle with HBSS EDTA and HBSS with collagenase as with the liver. Kidneys were removed and incubated for an additional 5–10 min to enhance digestion before proceeding with the above protocol. The endothelial cell-depleted fraction in the flow-through of the column was also collected. RNA was prepared immediately after cell isolation.

Growth and survival assays

For proliferation assays, passage-1 LSEC were starved overnight in 0.1% BSA and 0.2% fetal calf serum (FCS). The following morning, VEGF (10 ng/ml), mEG-VEGF, or hEG-VEGF (10 nM each) was added. Ten hours later, 1 μ Ci/ml ³H-thymidine was added, and the incubation was continued for an additional 24 h. At the end of the assay, cells were rinsed twice with cold PBS, fixed in 10% trichloroacetic acid, washed with water, and then lysed in 400 μ l of 0.2 N NaOH. This lysate was evaluated in a Beckman (Fullerton, CA) LS5000TD Liquid Scintillation System. The experiments were replicated with three independent preparations of primary LSEC

cultures. A representative experiment is shown, and *error bars* represent SD. Proliferation assays with bovine adrenal cortex capillary endothelial (ACE) cells were performed as previously described (29).

To assess cell survival activity, passage-1 LSEC cultures were incubated for 48 h in basic media without growth factors supplemented with 0.2% FCS, plus or minus 10 ng/ml VEGF, 10 nM mEG-VEGF, or 10 nM hEG-VEGF. Media containing the full complement of serum (10% FCS), without additional growth factors, were used for positive control. After 48 h, cells were harvested, fixed in 70% ethanol, and incubated at 4°C for at least 4 h with propidium iodide. The cell cycle distribution was assessed by fluorescence-activated cell sorting analysis. The sub-G1 population represented apoptotic cells and was determined using the Mcycle program. A representative experiment of duplicate samples is shown. *Error bars* represent SD.

Immunoblotting

Passage-1 primary LSEC cultures were starved overnight in media containing only 0.1% BSA and 0.2% FCS. The following morning, media were replaced with that containing only BSA for an additional 90 min. A total of 10 ng/ml VEGF, 20 nM EG-VEGF, or 20 nM hEG-VEGF was added, and incubations proceeded for 10 (ERK) or 15 (Akt) minutes before cells were quickly rinsed twice in cold PBS and lysed in 0.6 ml RIPA buffer (150 mM NaCl, 1% Nonidet P-40, 0.5% sodium orthovanadate, 50 mM Tris, pH 8.0) containing a protease inhibitor mixture (Roche,

Indianapolis, IN; MB 1836145) and phosphatase inhibitor cocktail (Sigma). Immunoblotting for phosphorylated ERK and Akt were performed as previously described (30). These experiments were performed with three independent preparations of primary LSEC.

Results

Mouse EG-VEGF cDNA

Ten cDNA clones were isolated from a mouse kidney cDNA library and sequenced. Although the 3' end of the cDNA corresponding to nucleotides 172–417 (Fig. 1A) and a long 3' untranslated region was intact, the 5' end of all clones isolated exhibited a high degree of heterogeneity, with the 5'-most sequence apparently derived from sequences within the first intron. A genomic fragment, identified from the mouse Sv129J BAC library at Research Genetics, Inc., was isolated and sequenced in its entirety. Clearly, exon 1 was present, encoding the predicted signal peptide and first five amino acids (aa) of the mature protein. A probe corresponding to the exon 1 sequence was amplified and used to screen a mouse tissue mRNA Northern blot. This fragment hybrid-

FIG. 1. The sequence of mEG-VEGF cDNA and predicted amino acid sequences are highly homologous to the human sequences. The predicted amino acid sequence of mEG-VEGF is shown with the corresponding nucleotide sequence of the cDNA isolated from a kidney library (A). B, Comparison of hEG-VEGF and mEG-VEGF amino acid sequences revealed 88% identity and 93% homology in the predicted mature protein. The signal peptides are 73% homologous.

A

```
GAAGTGAGGGGTACCAAAGTAGACTGTGTTTGTGTCACCTCAAGTGATC
ATGAGAGCGCTGTGCATATCTTCATCATGCTCCTTCTAGCAACGGCGTC
M R G A V H I F I M L L L A T A S
CGACTGTGCGGTACATCAGGGGCTGTGAACGAGATATCCAGTGTGGGG
D C A V I T G A C E R D I Q C G A
CCGGCACCTGCTGCGCTATCAGTCTGTGGCTGCGGGGCTGCGGTTGTGT
G T C C A I S L W L R G L R L C
ACCCCACTGGGGCGTGAAGGAGAGGAGTGCCACCCAGGAAGCCACAAGAT
T P L G R E G E E C H P G S H K I
CCCCTTCTTGAGGAAACGCCAACACCATACCTGTCCCTGCTCACCCAGCC
P F L R K R Q H H T C P C S P S L
TGCTGTGCTCCAGGTTCCCGACGGCAGGTACCGCTGCTTCCGGGACTTG
L C S R F P D G R Y R C F R D L
AAGAATGCCAACTTTTAGTTTGTCTGGAAGTCTGTCTGGAGCCTGACTGGG
K N A N F *
```

```
TGACCTCTTGCTTTACACCTGTGTGATTTAGCTCCCTGCAACTTCGCCAT
TCCCCATCTTGTCGGTGTATGTGCAGACAGGCAGACCTTCCGCTATGGAA
TAGTTACACAGGGTGCAGAGAGGAGTTCGTGGCCTTGAGAAGTTGGCCAG
CCCGACCTTCTGGCTCAGACTGCCTGAAGTTGTGACAGTGTGGGCCTTC
TCAGTTGCCTGCCCCCTTCCTGCATGTGCGCTTCTTCTAAACCAACACTT
TCTGGGCACTGGCCCATGGATGCACCACTAAATCAACAGGTCTGTGGGGT
GGATGATCAACTTTCTCTCCATTTTCTTTTATTGACTGGCTTCTTAATT
TAAGGACTGT....
```

B

```
MRGATRVSIMLLLVTVSDCAVITGACERDVQCGAGTCCAISLWLRGLRMC 50 hEG-VEGF
MRGAVHIFIMLLLATASDCAVITGACERDIQCGAGTCCAISLWLRGLRLC 50 mEG-VEGF
```

```
TPLGREGECHPGSHKVPFFRKRKHHTCPCLPNLLCSRFPDGRYRCMDL 100
TPLGREGECHPGSHKIPFLRKRQHHTCPCSPSLLCSRFPDGRYRCFIDL
```

```
KNINF 105
KNANF
```

ized a single band, corresponding to that hybridized by the incomplete cDNA clone, indicating that the sequences within this exon were coding for transcript. To further verify this conclusion, RT-PCR with a forward primer derived from exon 1 sequence revealed the expected product from kidney, liver, or d-7 embryo total RNA (see the supplemental data, published on The Endocrine Society's Journals Online web site at <http://endo.endojournals.org>). This product was not obtained using RNA samples from ovary and testis, consistent with little or no EG-VEGF mRNA expression in these tissues. The cDNA sequence of mEG-VEGF encodes a predicted peptide of 105 residues (Fig. 1). A well defined signal peptide of 19 aa is present, and therefore the mature mEG-VEGF protein is predicted to be 86 aa in length with a molecular mass of approximately 9 kDa. The mature mouse peptide is 88% identical and 93% homologous to the human protein. The signal sequences are also 73% conserved. Like the human molecule, we predict mEG-VEGF adopts a colipase fold (17), given that the span of the 10-cysteine residues conforms to the related snake peptide, the nuclear magnetic resonance structure of which was solved (31).

Gene structure

mEG-VEGF maps to a region of chromosome 3 syntenic with human chromosome 1p13.1, the locus for *hEG-VEGF*, providing further evidence that these genes are orthologs. Based on Southern hybridization to the mouse cDNA probe, two *HindIII* fragments were cloned from mouse BAC library

DNA preparations. One of the *HindIII* genomic fragments was 11 kb in length and contained more than 5 kb of promoter sequence and the first two exons. The second subclone included the exon 3 coding region and a long 3' UTR. The intron/exon borders of the human and mouse genes are absolutely conserved. Exon 1 encodes the 19 aa of the signal peptide and the first 5 residues of the mature protein (Fig. 2). The 6-aa changes within this exon are restricted to the coding sequence for the secretion signal. Exon 2 encodes 42 aa, including 6 of the 10 cysteines that are structural determinants of the colipase motif. Exon 3 encodes the remaining 39 aa, including 4 cysteines. Relative to human, 8 aa vary in this exon, and 3 of these represent conservative changes.

The first –2500 nt of the mEG-VEGF promoter are illustrated in Fig. 3A. The most striking feature is the presence of a TATA element that is not present in the human sequence. We examined the first –5000 nt of the human and mEG-VEGF promoters for regions of conservation. In this sequence, 3 discrete blocks of identity (80, 86, and 100%) represent only 262 nt of 5000, or 5.2% (Fig. 3, A and B). Given the very distinct expression of human EG-VEGF by steroidogenic tissues, we searched for steroid response elements within these –5000-nt regions. We identified a consensus steroidogenic factor (SF)-1 or NR5A1 (32) binding site at –1327 of the human, and not within the mouse, promoter. NR5A1 is an orphan nuclear receptor that regulates multiple target genes involved in gonadal and adrenal determination and development, steroidogenesis, and reproduction. NR5A1 binds to target promoters as a monomer and recognizes

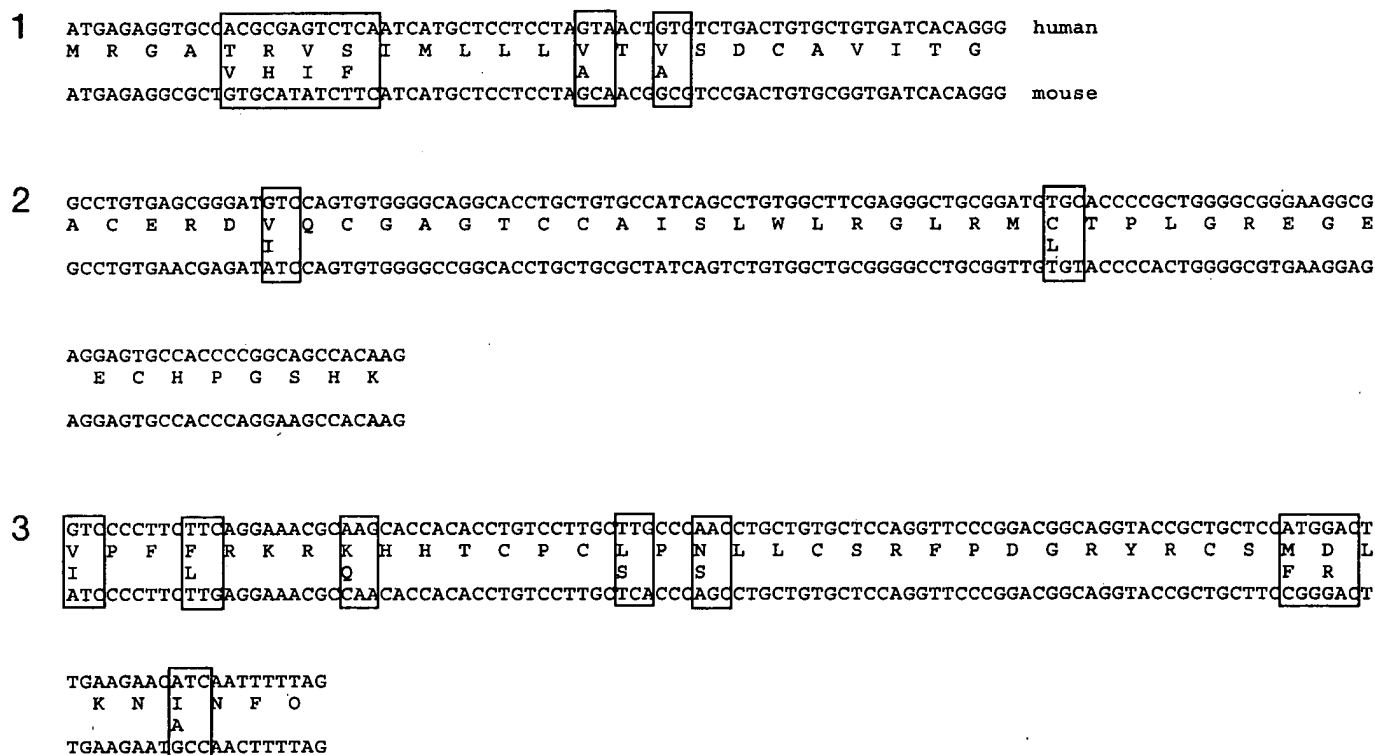


FIG. 2. The genomic structures of human and mouse EG-VEGF are conserved. Alignment of the intron/exon boundaries of the human and mouse genomic sequences revealed the highly conserved organization. Exon 1 contains the coding sequences for the signal peptide and the first 5 aa of the mature protein. Exon 2 encodes 6 of 10 cysteines and 42 residues in total, and exon 3 the remaining 49 aa. Differences in nucleotide sequence between mouse and human are boxed.

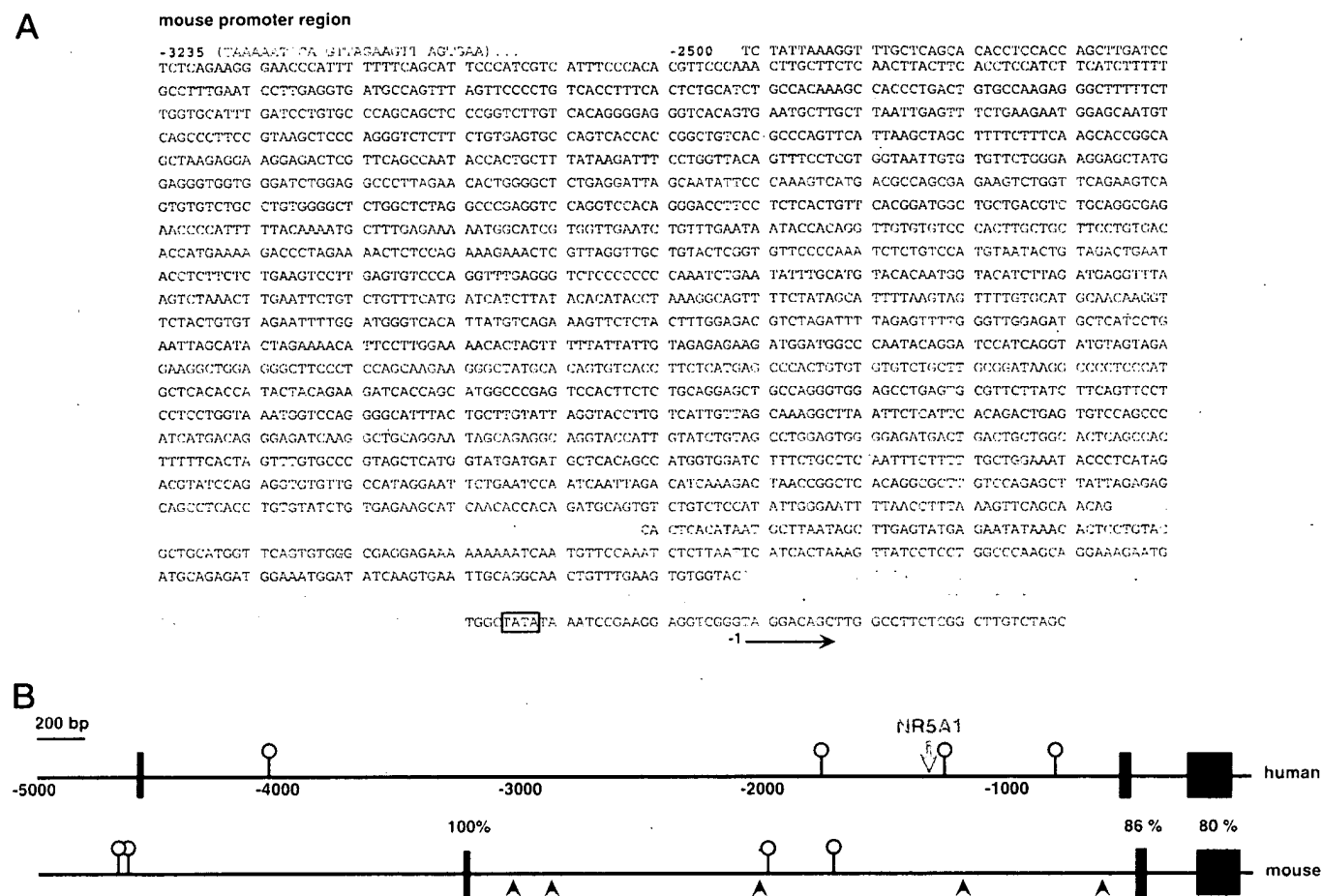


FIG. 3. The human and mouse EG-VEGF promoter sequences are divergent. **A**, Illustrated is -2.5 kb of the mouse promoter sequence. The -1 position is indicated with the start of transcription, the TATA element is boxed, and the sequence in red accounts for blocks of high conservation with the human promoter. **B**, Comparison of the -5.0 -kb region of human and mouse promoters is presented. The three blocks of 80–100% conservation are illustrated. A unique NR5A1/SF-1 site (arrow) in the human promoter potentially localizes expression to steroidogenic cells. Importantly, this sequence is not conserved between the human and mouse promoters. The location of putative hypoxia response elements (circles) and C/EBP consensus sites (arrowheads) are illustrated.

an extended half-site motif designated PyCA AGGTCA. The corresponding sequence in the human promoter is TCA AGGTCA (Fig. 3B). CCAAT enhancer binding proteins (C/EBPs) are a family of liver-enriched transcription factors (33, 34). Within the mouse promoter, we identified five C/EBP binding sites (-3037 , -2891 , -2033 , -1189 , and -621 nt). One site is present in the human promoter (-393). Several molecules, including angiogenic factors, are induced by low oxygen tension via the hypoxia-inducible factor, HIF-1 α (35). Based on the consensus sequence, TA CGTG CGGC (bold sequence invariable), putative hypoxia regulatory elements are located at -4052 , -1773 , -1263 , and -811 in the human promoter and at -4651 , -4690 , -2014 , and -1743 in the mouse. Apparently, the divergence of promoter sequence between human and mouse accounts for the selective and unique expression patterns.

Expression profile of mEG-VEGF mRNA: comparison with Bv8 and VEGF-A

Northern blot analysis of mRNA from a variety of mouse tissues indicated that a single transcript of approximately 3.5

kb was restricted to kidney and liver (Fig. 4A). This size is considerably larger than the human transcript (1.4 kb), due to a longer 3' untranslated region (data not shown). In agreement with these data, kidney and liver express relatively high levels of EG-VEGF transcript as assessed by Taqman analysis. Very low levels of mEG-VEGF are expressed in lung and testis, and the transcript is essentially undetectable in the ovary (Fig. 4B). The highest expression is detected in RNA samples from embryonic d 7 (Fig. 4B). Notably, d 7 encompasses the period of gastrulation, which gives rise to the mesoderm. We also examined the expression of the EG-VEGF homolog, Bv8, in the same RNA samples. Bv8 expression was detected in testis, prostate, and ovary, suggesting that in the rodent, Bv8 may, at least in part, assume functions we proposed for human EG-VEGF within these tissue contexts (Fig. 4C; Ref. 22). The expression pattern of VEGF-A was also determined. VEGF was widely distributed, with highest levels in kidney, liver, ovary, and prostate, and a weaker signal in lung, heart, brain, and embryonic d 7 embryo samples (Fig. 4D).

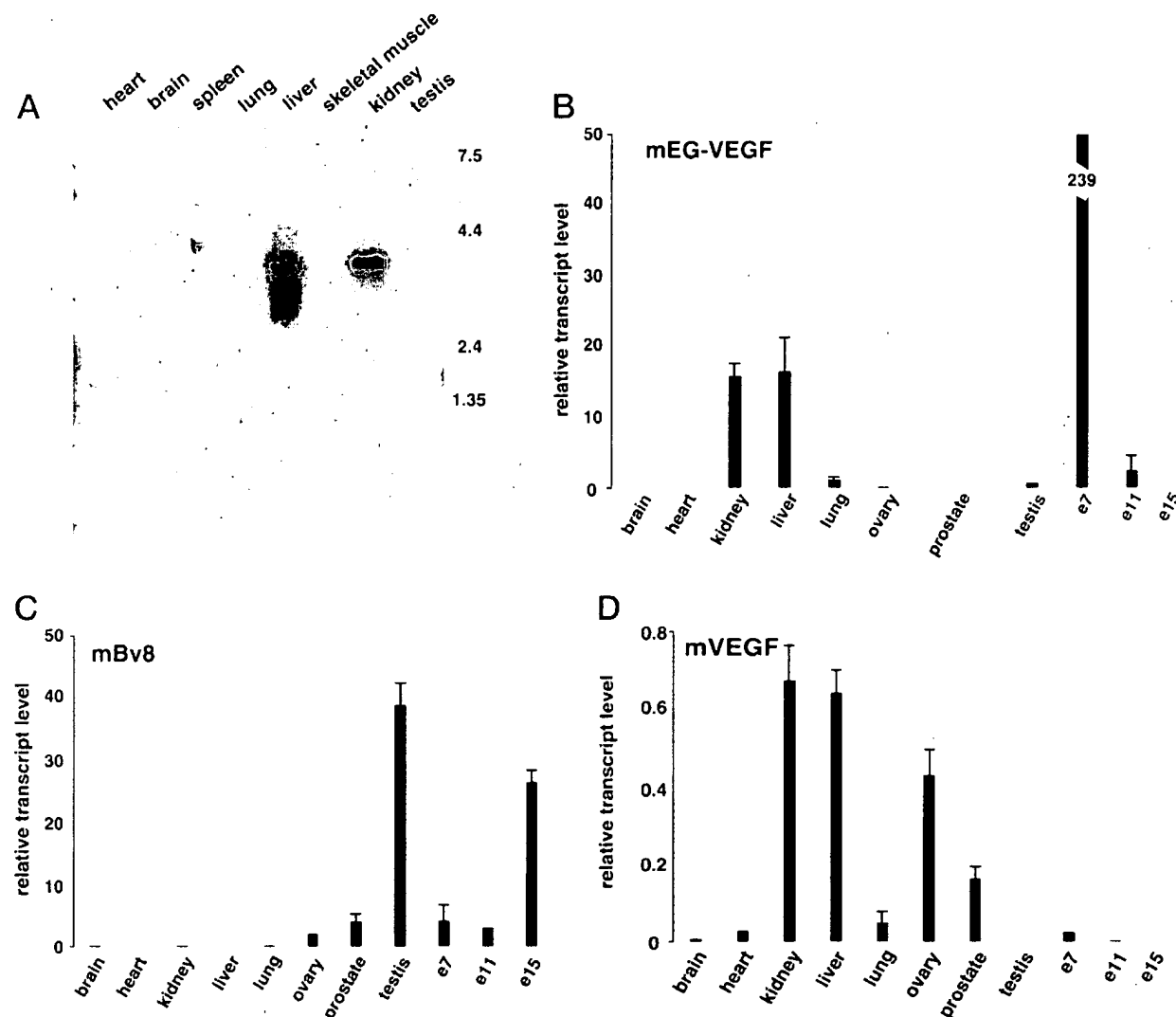


FIG. 4. The predominant sites of mouse EG-VEGF expression are liver and kidney. Northern blot analysis of poly adenosine-selected mouse RNA revealed a single band at approximately 3.5 kb in liver and kidney samples (A). Lane contents and relative transcript size (kb) are indicated. B, Taqman analysis of an extended panel of mouse tissue RNA samples revealed that, in addition to high levels of transcript in liver and kidney, mEG-VEGF is highly expressed in the d-7 embryo (broken bar, value is indicated). Low levels were detected in lung, testis, older embryos, and ovary. The relative transcript levels of the related peptide, mBv8 (C), and mVEGF-A (D) were also determined in these samples. mBv8 appears to have a fundamentally nonoverlapping pattern of expression compared with mEG-VEGF. Tissues expressing mBv8 transcript include testis, prostate, and ovary, as well as d-15 embryos. The highest relative levels of VEGF-A transcript are found within kidney, liver, ovary, and prostate, partially overlapping the mEG-VEGF and Bv8 expression patterns.

Localization of mEG-VEGF mRNA by *in situ* hybridization

We performed *in situ* hybridization studies using a panel of mouse tissues that included embryo, brain, liver, kidney, lung, pancreas, spleen, large and small intestine, lymph node, prostate, testis, and adrenal gland. In agreement with the Northern and Taqman analysis, specific signal was detected only in liver and kidney. In the d-18 embryo, the fetal liver expresses a very high level of EG-VEGF transcript, with signal restricted to hepatocytes (Fig. 5, A–C). In the adult liver, this signal is reduced (data not shown). In the adult kidney, the specific hybridization signal is restricted to the epithelial tubule cells, with no signal present in the glomeruli (Fig. 5, D and E).

Tissue distribution of mEG-VEGF receptors

We wished to evaluate the expression of the two EG-VEGF receptors, R-1 and R-2, in a variety of tissues. Taqman analysis revealed a partially overlapping distribution of these receptors. R-1 expression was predominantly in samples from prostate, ovary, testis, and d-15 embryo. As illustrated in Fig. 6, R-2 was detected in a broader pattern, being highest in brain, prostate, d-7 embryo, liver, ovary, testis, and kidney.

Expression of EG-VEGF receptors in endothelial cells from liver and kidney

RNA was prepared from total liver or total kidney and also from distinct preparations of hepatocytes, purified LSEC,

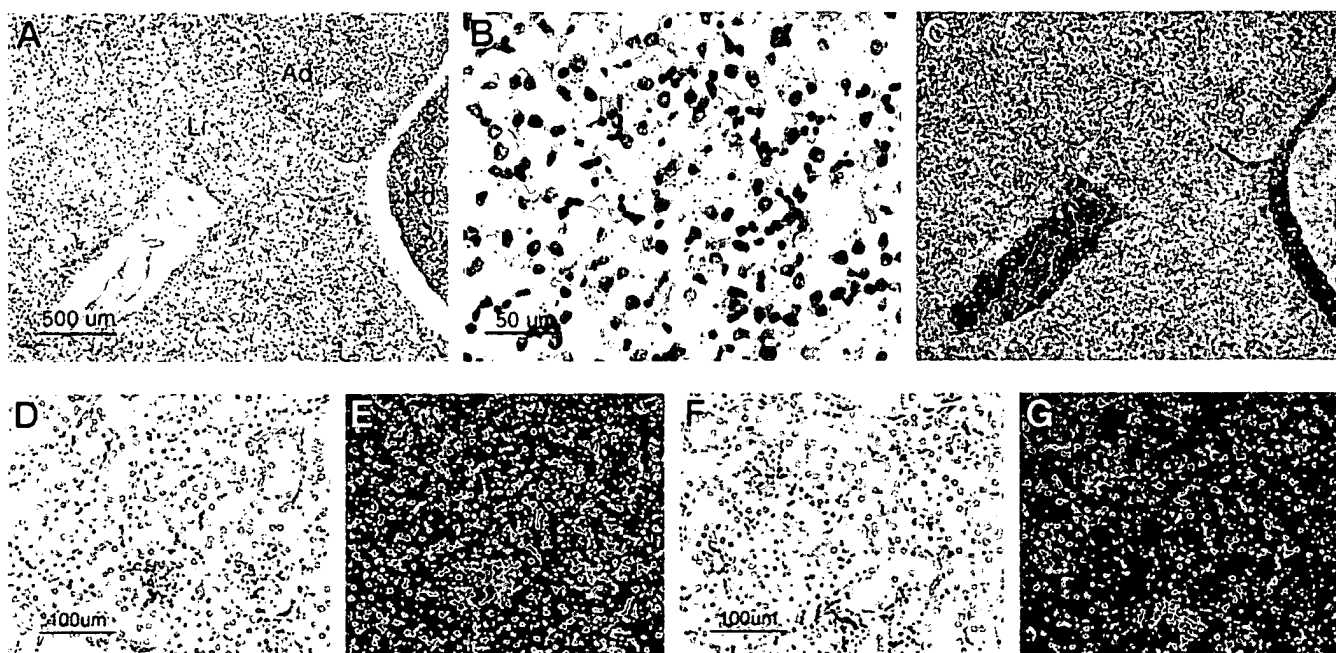


FIG. 5. mEG-VEGF mRNA expression is restricted to hepatocytes and tubule cells in the kidney. *In situ* hybridization analyses revealed that in the fetal mouse liver, EG-VEGF is restricted to and highly expressed in hepatocytes. Note the signal associated with the parenchyma cells in the bright-field images (A and B, inset at higher magnification) and the companion dark-field image (C). Note the absence of signal in the adjacent fetal adrenal gland (Ad) and section of kidney (Kd). In the adult kidney, the hybridization signal is associated with the tubule (Tb) cells as illustrated in the bright- and dark-field images (D and E) and not the glomeruli (Gl). Lack of specific hybridization signal of the control sense probe is shown for kidney sections (F and G). Magnification is indicated.

and endothelial cell-depleted and purified endothelial cells from kidney, as described in *Materials and Methods*. These samples were submitted to Taqman analysis for the ligand and the putative receptors. In agreement with the *in situ* hybridization data, the mEG-VEGF transcript is expressed in the hepatocyte fraction (Fig. 6B) or the endothelial cell-depleted kidney fraction (Fig. 6D), whereas it is almost undetectable in purified endothelial cells from both organs. Conversely, the expression of EG-VEGFR-2 was associated with the purified LSEC or endothelial cells from kidney (Fig. 6, C and E). EG-VEGFR-1 expression was undetectable in these samples.

mEG-VEGF is a mitogen and survival factor for endothelial cells

Previously, we have reported that hEG-VEGF displays mitotic and prosurvival activity toward target ACE cells (30). We confirmed that mEG-VEGF also induced proliferation of ACE cells (Fig. 7A). Therefore, we sought to test whether the mouse ortholog was also capable of such activity using the presumably physiologically relevant target cell in our bioassays. Proliferation experiments were performed using primary LSEC. ³H-Thymidine incorporation assays revealed that, like VEGF (2.70-fold increase in thymidine incorporation), either recombinant mEG-VEGF (2.1-fold induction) or hEG-VEGF (1.94-fold) stimulated proliferation of the LSEC cultures (Fig. 7B). Consistent with this activity, addition of VEGF, mEG-VEGF, or hEG-VEGF to LSEC cultures resulted in a robust phosphorylation of MAPK ERK-1/2 within 10 min of ligand addition (Fig. 7C). A second activity we have

previously ascribed to hEG-VEGF is the ability to act as a survival factor for ACE cells (30). The ability of mEG-VEGF to promote survival of LSECs was assessed by determining the fraction of apoptotic cells following a 48-h incubation in 0.2% FCS with or without exogenous ligand. LSEC cultures incubated in 0.2% FCS-containing media reproducibly exhibited $30 \pm 5.5\%$ apoptotic cells (Fig. 7D). Addition of 10 ng/ml VEGF inhibited the cell death, significantly reducing the percentage of apoptotic cells to $8 \pm 2.7\%$; 10 nM mEG-VEGF reduced cell death to $10 \pm 4\%$; and hEG-VEGF was equivalent to the mouse ligand in these assays, $13.4 \pm 2.2\%$ apoptotic cells. Activation of the survival, phosphatidylinositol-3 kinase/Akt intracellular signaling pathway was assessed with an Akt phosphorylation specific antibody. Within 15 min of stimulation with VEGF or EG-VEGF, there was a marked increase in the level of phosphorylated Akt (Fig. 7E). Based on these findings, we conclude that mEG-VEGF is a mitogen and survival factor for endothelial cells.

Discussion

We describe herein the cloning of the mouse EG-VEGF cDNA and genomic locus and the mRNA tissue distribution. Our interest in this molecule stems from our identification of hEG-VEGF as an angiogenic factor with selective activity. Given the power of mouse molecular genetics, we sought to establish the reagents to further examine the biology and *in vivo* functions of the mouse ortholog to gain further insight into the biology of EG-VEGF. The mouse EG-VEGF gene encodes a mature 86-residue peptide that is 88% identical and 93% homologous to the human protein. The gene struc-

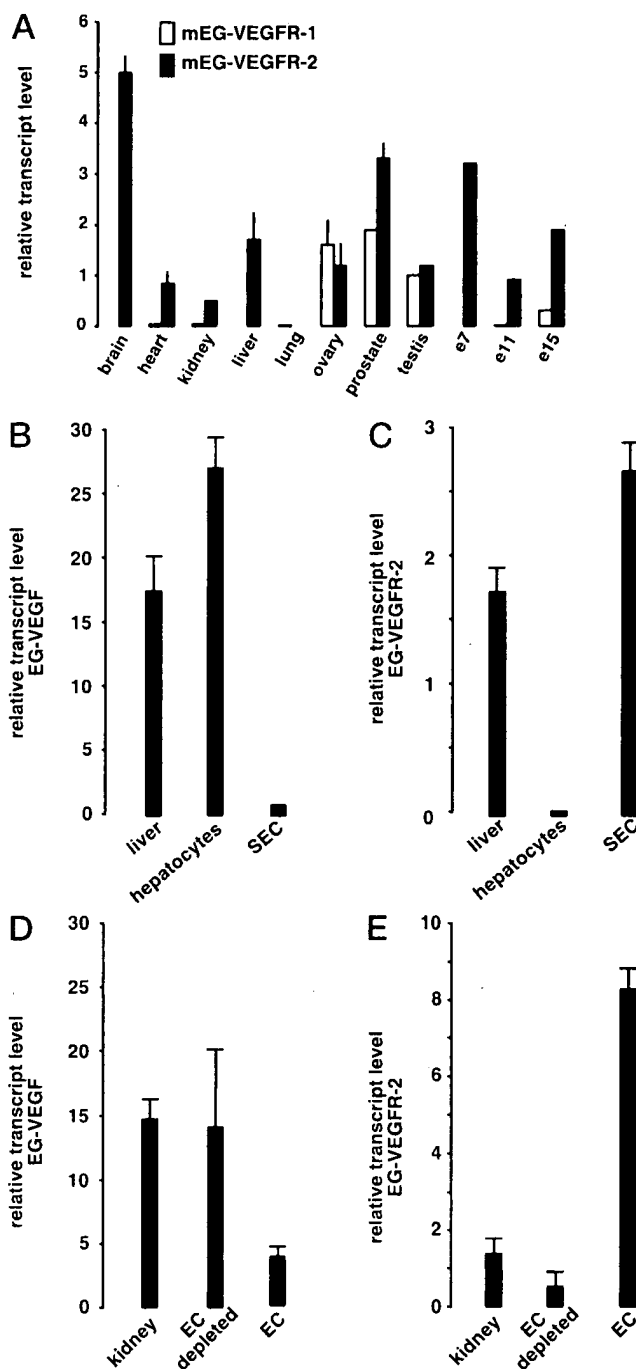


FIG. 6. Distribution of EG-VEGFR-1 (R1) and EG-VEGFR-2 (R2) mRNA in various tissues and selective expression of R2 mRNA in LSEC and kidney endothelial cells. A, Taqman analysis for EG-VEGF receptors was examined in a panel of mouse tissues and staged embryos. R-1 transcripts were detected in ovary, prostate, and testis and also at embryonic d 15. EG-VEGFR-2 is highly expressed in brain and prostate and throughout the period of embryonic development at d 7–15. The R-2 transcript is also expressed in liver, kidney, ovary, testis, and heart. B and C, The mEG-VEGF transcript is associated with the purified hepatocyte fraction, whereas expression of the receptor, EG-VEGFR-2, is restricted to the LSEC fraction. D and E, Transcript for the ligand is highest in the total kidney or endothelial-cell depleted kidney preparations, but the EG-VEGFR-2 mRNA is highest in kidney endothelial cells. Representative experiments are shown.

ture is also conserved between man and mouse. The predominant sites of mEG-VEGF expression are the liver and kidney. We determined that EG-VEGF stimulated proliferation and survival of primary LSEC. Furthermore, we detected EG-VEGFR-2 expression in endothelial cells, but not in other cell types, within liver and kidney. This finding is in agreement with recent *in situ* hybridization studies showing that, in the mouse testis, EG-VEGF receptors are localized to vascular endothelial cells (22). Therefore, similar to VEGF and its receptors (36), the EG-VEGF/EG-VEGFR system appears to function in a paracrine fashion, as the ligand is produced by nonendothelial cells and the receptors are selectively expressed in the vascular endothelium.

Interestingly, the ultrastructural features of capillary endothelial cells within the liver (37) and kidney are similar to those of the endocrine glands (38). Hence, we propose that, similar to hEG-VEGF, mEG-VEGF may influence the phenotype and growth properties of endothelial cells in distinct tissue compartments enriched in fenestrated endothelium.

Of particular interest is the difference in expression pattern between mouse and human, in which it is largely restricted to steroidogenic cells within ovary, testis, adrenal, and placenta (12). In the human and primate ovary, a seemingly dynamic EG-VEGF expression pattern led to the proposal that angiogenesis in the developing follicle and corpus luteum may be coordinated by the complementary activities of EG-VEGF and VEGF (39). Why this difference in expression pattern between mouse and human? A comparison of the human and mouse promoters revealed little conservation. Strikingly, a perfect consensus site for NR5A1 (also SF-1) binding (32) is present in the hEG-VEGF but not mEG-VEGF promoter sequence. NR5A1, an orphan nuclear receptor, is considered a key regulator of endocrine development and function. This transcription factor was originally identified based upon its ability to interact with a promoter element in genes encoding the cytochrome P450 hydroxylases (40, 41) and its restricted expression in adrenal cortical cells, testicular Leydig, ovarian theca, and granulosa cells (42) and placenta (40). Gene-targeting studies revealed a critical role for SF-1/NR5A1 in adrenal and gonad development (43, 44). In the adult ovary, NR5A1 protein expression is recognized at the onset of follicular development and is strongly induced within antral follicles in theca and granulosa cells (45). The parallels between the known expression and activity of NR5A1 and the expression profile of hEG-VEGF leads us to propose that NR5A1 may be potentially important in regulating transcription of the human EG-VEGF gene. Site-directed mutagenesis of this element within the human EG-VEGF promoter will be required to verify this hypothesis. Likewise, verification of the role of other putative regulatory elements, C/EBP and hypoxia response element, identified in the mouse promoter requires a mutagenesis-based analysis. Although a homolog of NR5A1, NR5A2/LRH-1 (46), is expressed in the liver, the mouse gene promoter does not include the canonical target sequence for this factor.

Although the mouse or rat is a commonly used model, there are major differences in ovarian physiology between rodents and humans, or the higher primates. In humans and other primates, a single follicle, referred to as the dominant follicle, is typically selected from the cohort that enters the

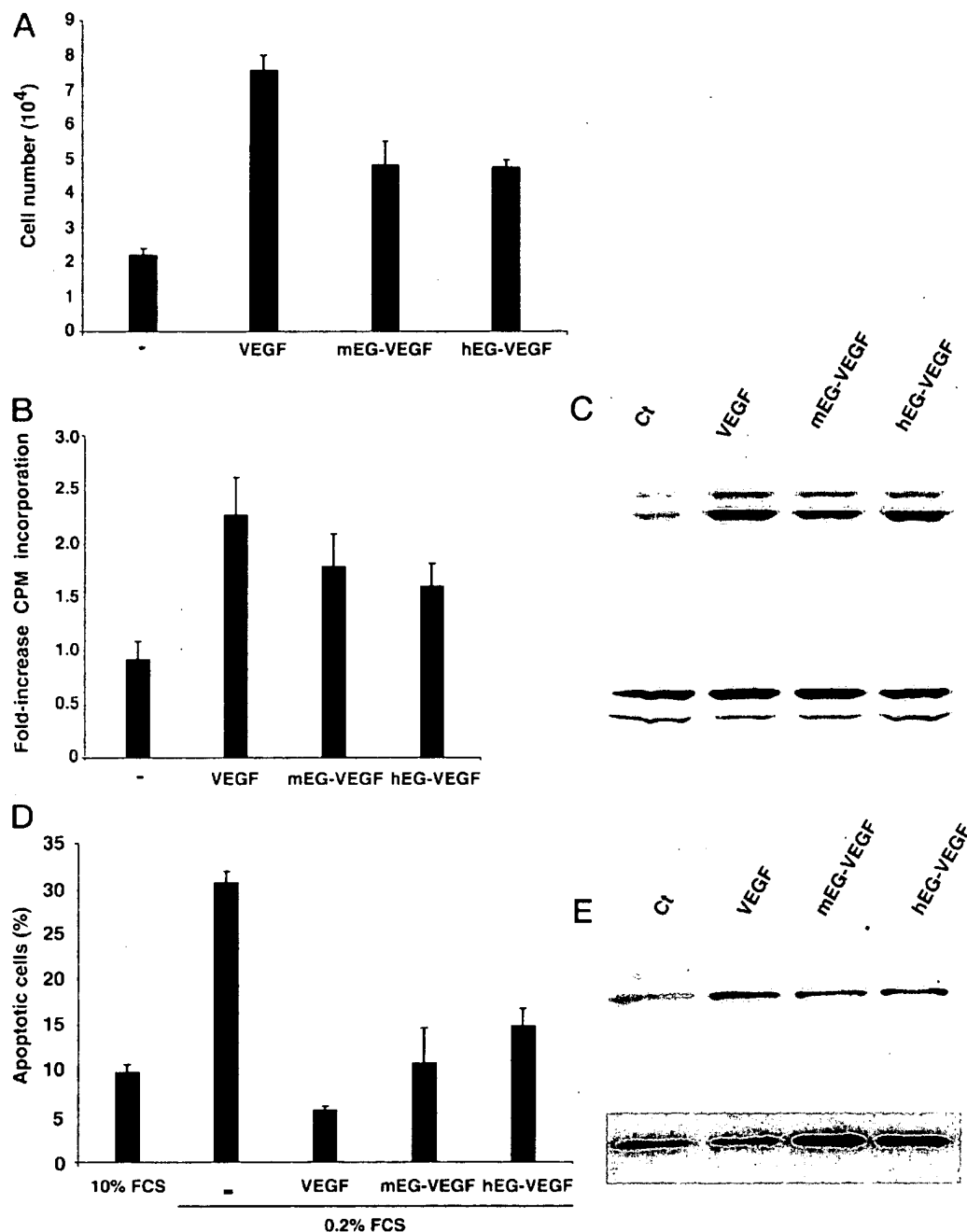


FIG. 7. Mouse EG-VEGF is an endothelial cell mitogen and survival factor. A, mEG-VEGF and hEG-VEGF induced comparable increases in ACE cell number. B, mEG-VEGF, hEG-VEGF, or VEGF induced a significant increase in ^3H -thymidine incorporation in LSEC cultures. C, mEG-VEGF, hEG-VEGF, and VEGF all induced comparable levels of phosphorylation of ERK1 and -2 proteins in LSEC cultures after a 10-min stimulation. The immunoblot for total ERK1/2 proteins is presented as loading control. D, mEG-VEGF, hEG-VEGF, or VEGF markedly inhibited LSEC apoptosis induced by low serum conditions. Ten percent FCS served as positive control for cell survival. E, Phosphorylation of the prosurvival Akt signaling molecule increased after a 15-min stimulation with VEGF, mEG-VEGF, or hEG-VEGF. Total Akt protein levels were analyzed in the lower panel for loading control.

follicular cycle (47, 48). In these and other monovular species, this single follicle deviates from the others, establishes dominance, and it alone may be competent to achieve ovulation. The development of a more elaborate capillary network is expected to provide a growth and survival advantage to the dominant follicle (49). Further studies are required to deter-

mine whether EG-VEGF plays a role in this process. We recently found that, whereas EG-VEGF mRNA expression is not detectable in early-stage human corpus luteum, it is up-regulated during mid through early late luteal phase, at a time when VEGF expression is much reduced or undetectable (50). Perhaps a greater length of the ovarian cycle

(28 d in humans vs. 4 d in mice and rats) requires a more complex regulation of growth and maintenance of the vascular endothelium during follicular and luteal phases. It is tempting to speculate that EG-VEGF represents one growth factor component that contributes to these evolutionary changes. Interestingly, human EG-VEGF is highly expressed in the polycystic ovary syndrome (50), a leading cause of infertility associated with hyperplasia of ovarian stroma and angiogenesis (51). This disorder occurs in humans but not in rodents. It will be interesting to determine when, on an evolutionary scale, EG-VEGF expression first became associated with the ovary and other steroidogenic tissues.

The fact that EG-VEGF and Bv8 appear to bind and activate EG-VEGFR-1 or EG-VEGFR-2 equivalently and have indistinguishable biological effects (22, 24) raises the possibility that, in the mouse, Bv8 may serve at least some of the functions previously proposed for hEG-VEGF. In the mouse, Bv8 is expressed in testis, prostate, and at lower but still significant levels in the ovary. Thus, mEG-VEGF and mBv8 appear to exhibit nonoverlapping tissue distributions, indicating that the two peptides may potentially have related functions in their distinct/unique contexts. The distribution of the EG-VEGF receptors supports this possibility (23, 24). Mouse R-2 has a broader spectrum of expression than R-1, although the two receptors appear to be almost equally expressed in ovary, testis, as well as prostate. Potentially, experiments in genetically modified mice may further test hypotheses regarding the role of the EG-VEGF ligand/receptor system in endothelial cell biology, in addition to identifying distinct functions in other cell and tissue contexts.

Acknowledgments

We thank J. Lee for cDNA libraries.

Received December 16, 2002. Accepted March 3, 2003.

Address all correspondence and requests for reprints to: Napoleone Ferrara, M.D., Genentech, Inc., Department of Molecular Oncology, 1 DNA Way, South San Francisco, California 94080. E-mail: nf@gene.com.

References

- Risau W 1997 Mechanisms of angiogenesis. *Nature* 386:671–674
- Folkman J 1995 Angiogenesis in cancer, vascular, rheumatoid and other disease. *Nat Med* 1:27–31
- Ferrara N, Carver-Moore K, Chen H, Dowd M, Lu L, O'Shea KS, Powell-Braxton L, Hillan KJ, Moore MW 1996 Heterozygous embryonic lethality induced by targeted inactivation of the VEGF gene. *Nature* 380:439–442
- Carmeliet P, Ferreira V, Breier G, Pollefeyt S, Kieckens L, Gertsenstein M, Fahrig M, Vandenhoek A, Harpal K, Eberhardt C, Declercq C, Pawling J, Moons L, Collen D, Risau W, Nagy A 1996 Abnormal blood vessel development and lethality in embryos lacking a single VEGF allele. *Nature* 380:435–439
- Suri C, Jones PF, Patan S, Bartunkova S, Maisonnier PC, Davis S, Sato TN, Yancopoulos GD 1996 Requisite role of angiopoietin-1, a ligand for the TIE2 receptor, during embryonic angiogenesis. *Cell* 87:1171–1180
- Maisonnier PC, Suri C, Jones PF, Bartunkova S, Wiegand SJ, Radziejewski C, Compton D, McClain J, Aldrich TH, Papadopoulos N, Daly TJ, Davis S, Sato TN, Yancopoulos GD 1997 Angiopoietin-2, a natural antagonist for Tie2 that disrupts in vivo angiogenesis. *Science* 277:55–60
- Fong GH, Rossant J, Gertsenstein M, Breitman ML 1995 Role of the Flt-1 receptor tyrosine kinase in regulating the assembly of vascular endothelium. *Nature* 376:66–70
- Shalaby F, Rossant J, Yamaguchi TP, Gertsenstein M, Wu XF, Breitman ML, Schuh AC 1995 Failure of blood-island formation and vasculogenesis in Flk-1-deficient mice. *Nature* 376:62–66
- Dumont DJ, Gradwohl G, Fong GH, Puri MC, Gertsenstein M, Auerbach A, Breitman ML 1994 Dominant-negative and targeted null mutations in the endothelial receptor tyrosine kinase, tek, reveal a critical role in vasculogenesis of the embryo. *Genes Dev* 8:1897–1909
- Kolonin MG, Pasqualini R, Arap W 2001 Molecular addresses in blood vessels as targets for therapy. *Curr Opin Chem Biol* 5:308–313
- Arap W, Kolonin MG, Trepel M, Lahdenranta J, Cardo-Vila M, Giordano RJ, Mintz PJ, Ardelt PU, Yao VJ, Vidal CI, Chen L, Flamm A, Valtanen H, Weavind LM, Hicks ME, Pollock RE, Botz GH, Bucana CD, Koivunen E, Cahill D, Troncoso P, Baggerly KA, Pentz RD, Do KA, Logothetis CJ, Pasqualini R 2002 Steps toward mapping the human vasculature by phage display. *Nat Med* 8:121–127
- LeCouter J, Kowalski J, Foster J, Hass P, Zhang Z, Dillard-Telm L, Frantz G, Rangell L, DeGuzman L, Keller G-A, Peale F, Gurney A, Hillan KJ, Ferrara N 2001 Identification of an angiogenic nitroselective for endocrine gland endothelium. *Nature* 412:877–884
- Glinka A, Wu W, Delius H, Monaghan AP, Blumenstock C, Niehrs C 1998 Dickkopf-1 is a member of a new family of secreted proteins and functions in head induction. *Nature* 393:357–362
- Joubert FJ, Strydom DJ 1980 Snake venom. The amino acid sequence of protein A from *Dendroaspis polylepis polylepis* (black mamba) venom. *Hoppe Seyler's Z Physiol* 361:1787–1794
- Schweitz H, Pacaud P, Diocot S, Moinier D, Lazdunski M 1999 MIT(1), a black mamba toxin with a new and highly potent activity on intestinal contraction. *FEBS Lett* 461:183–188
- Mollay C, Wechselberger C, Mignogna G, Negri L, Melchiorri P, Barra D, Kreil G 1999 Bv8, a small protein from frog skin and its homologue from snake venom induce hyperalgesia in rats. *Eur J Pharmacol* 374:189–196
- Aravind L, Koonin EV 1998 A colipase fold in the carboxy-terminal domain of the Wnt antagonists—the Dickkops. *Curr Biol* 8:R477–R478
- Wechselberger C, Puglisi R, Engel E, Leppendinger G, Boitani C, Kreil G 1999 The mammalian homologues of frog Bv8 are mainly expressed in spermatocytes. *FEBS Lett* 462:177–181
- Li M, Bullock CM, Knauer DJ, Ehler FJ, Zhou QY 2001 Identification of two prokineticin cDNAs: recombinant proteins potently contract gastrointestinal smooth muscle. *Mol Pharmacol* 59:692–698
- Melchiorri D, Bruno V, Besong G, Ngomba RT, Cuomo L, De Biasi A, Copani A, Moschella C, Storto M, Nicoletti F, Leppendinger G, Passarelli F 2001 The mammalian homologue of the novel peptide Bv8 is expressed in the central nervous system and supports neuronal survival by activating the MAP kinase/PI-3-kinase pathways. *Eur J Neurosci* 13:1694–1702
- Cheng MY, Bullock CM, Li C, Lee AG, Bermak JC, Belluzzi J, Weaver DR, Leslie FM, Zhou QY 2002 Prokineticin 2 transmits the behavioural circadian rhythm of the suprachiasmatic nucleus. *Nature* 417:405–410
- LeCouter J, Lin R, Tejada M, Frantz G, Peale F, Hillan KJ, Ferrara N 2003 The EG-VEGF homologue Bv8 promotes angiogenesis in the testis. Localization of Bv8 receptors to endothelial cells. *Proc Natl Acad Sci USA* 100:2685–2690
- Lin DC, Bullock CM, Ehler FJ, Chen JL, Tian H, Zhou QY 2002 Identification and molecular characterization of two closely related G protein-coupled receptors activated by prokineticins/endocrine gland vascular endothelial growth factor. *J Biol Chem* 277:19276–19280
- Masuda Y, Takatsu Y, Terao Y, Kumano S, Ishibashi Y, Suenaga M, Abe M, Fukusumi S, Watanabe T, Shintani Y, Yamada T, Hinuma S, Inatomi N, Ohtaki T, Onda H, Fujino M 2002 Isolation and identification of EG-VEGF/prokineticins as cognate ligands for two orphan G-protein-coupled receptors. *Biochem Biophys Res Commun* 293:396–402
- Phillips HS, Hains JM, Laramée GR, Rosenthal A, Winslow JW 1990 Widespread expression of BDNF but not NT3 by target areas of basal forebrain cholinergic neurons. *Science* 250:290–294
- Melton DA, Krieg PA, Rebagliati MR, Maniatis T, Zinn K, Green MR 1984 Efficient in vitro synthesis of biologically active RNA and RNA hybridization probes from plasmids containing a bacteriophage SP6 promoter. *Nucleic Acids Res* 12:7035–7056
- Harman AW, McCamish LE, Henry CA 1987 Isolation of hepatocytes from postnatal mice. *J Pharmacol Methods* 17:157–163
- LeCouter J, Moritz D, Li B, Lewis Phillips G, Liang X-H, Gerber HP, Hillan KJ, Ferrara N 2003 Angiogenesis-independent endothelial protection of liver: role of VEGFR-1. *Science* 299:890–893
- Leung DW, Cachianes G, Kuang WJ, Goeddel DV, Ferrara N 1989 Vascular endothelial growth factor is a secreted angiogenic mitogen. *Science* 246:1306–1309
- Lin R, LeCouter J, Kowalski J, Ferrara N 2002 Characterization of endocrine gland-derived vascular endothelial growth factor signaling in adrenal cortex capillary endothelial cells. *J Biol Chem* 277:8724–8729
- Boisbouvier J, Albrand JP, Blackledge M, Jaquinod M, Schweitz H, Lazdunski M, Marion D 1998 A structural homologue of colipase in black mamba venom revealed by NMR floating disulphide bridge analysis. *J Mol Biol* 283:205–219
- Parker KL, Rice DA, Lala DS, Ikeda Y, Luo X, Wong M, Bakke M, Zhao L, Frigeri C, Hanley NA, Stallings N, Schimmer BP 2002 Steroidogenic factor 1: an essential mediator of endocrine development. *Recent Prog Horm Res* 57:19–36
- Takiguchi M 1998 The C/EBP family of transcription factors in the liver and other organs. *Int J Exp Pathol* 79:369–391

34. Ramji DP, Foka P 2002 CCAAT/enhancer-binding proteins: structure, function and regulation. *Biochem J* 365:561–575
35. Semenza GL 2000 HIF-1: mediator of physiological and pathophysiological responses to hypoxia. *J Appl Physiol* 88:1474–1480
36. Ferrara N 2000 Vascular endothelial growth factor and the regulation of angiogenesis. *Recent Prog Horm Res* 55:15–35
37. Wisse E, Braet F, Luo D, De Zanger R, Jans D, Crabbe E, Vermoesen A 1996 Structure and function of sinusoidal lining cells in the liver. *Toxicol Pathol* 24:100–1111
38. Palade GE, Simionescu M, Simionescu N 1979 Structural aspects of the permeability of the microvascular endothelium. *Acta Physiol Scand (Suppl)* 463:11–32
39. LeCouter J, Lin R, Ferrara N 2002 Endocrine gland-derived VEGF and the emerging hypothesis of organ-specific regulation of angiogenesis. *Nat Med* 8:913–917
40. Honda S, Morohashi K, Nomura M, Takeya H, Kitajima M, Omura T 1993 Ad4BP regulating steroidogenic P-450 gene is a member of the steroid hormone receptor superfamily. *J Biol Chem* 268:7494–7502
41. Lala DS, Rice DA, Parker KL 1992 Steroidogenic factor I, a key regulator of steroidogenic enzyme expression, is the mouse homolog of fushi tarazu-factor I. *Mol Endocrinol* 6:1249–1258
42. Ikeda Y, Shen W-H, Ingraham HA, Parker KL 1994 Developmental expression of mouse steroidogenic factor I, an essential regulator of the steroid hydroxylases. *Mol Endocrinol* 9:478–486
43. Luo X, Ikeda Y, Parker KL 1994 A cell specific nuclear receptor is required for adrenal and gonadal development for male sexual differentiation. *Cell* 77:481–490
44. Sadovsky Y, Crawford P, Woodson K, Polish J, Clements M, Touretlote L, Simburger K, Milbrandt J 1995 Mice deficient in the orphan receptor steroidogenic factor 1 lack adrenal glands and gonads but express P450 side-chain-cleavage enzyme in the placenta and have normal embryonic serum levels of corticosteroids. *Proc Natl Acad Sci USA* 92:10939–10943
45. Takayama K, Sasano H, Fukaya T, Morohashi K, Suzuki T, Tamura M, Costa MJ, Yajima A 1995 Immunohistochemical localization of Ad4-binding protein with correlation to steroidogenic enzyme expression in cycling human ovaries and sex cord stromal tumors. *J Clin Endocrinol Metab* 80:2815–2821
46. Galanteau L, Pare JF, Allard D, Hamel D, Levesque L, Tugwood JD, Green S, Belanger L 1996 The α 1-fetoprotein locus is activated by a nuclear receptor of the Drosophila FTZ-F1 family. *Mol Cell Biol* 16:3853–3865
47. Hodgen GD 1982 The dominant ovarian follicle. *Fertil and Steril* 38:281–299
48. Ginther OJ, Beg MA, Bergfelt DR, Donadeu FX, Kot K 2001 Follicle selection in monovular species. *Biol Reprod* 65:638–647
49. Zeleznik AJ, Schuler HM, Reichert LEJ 1981 Gonadotropin-binding sites in the rhesus monkey ovary: role of the vasculature in the selective distribution of human chorionic gonadotropin to the preovulatory follicle. *Endocrinology* 109:356–362
50. Ferrara N, Frantz G, LeCouter J, Dillard-Telm L, Pham T, Draksharapu A, Giordano T, Peale F, Differential expression of the angiogenic factor genes VEGF and EG-VEGF in normal and polycystic human ovaries. *Am J Pathol*, in press
51. Strauss JFI, Dunaif A 1999 Molecular mysteries of polycystic ovary syndrome. *Mol Endocrinol* 13:800–805